Insertion of Amines and Alcohols into Proton-Bound Dimers. A Density Functional Study

Jan M. L. Martin,[†] Viktorya Aviyente,[‡] and Chava Lifshitz*[,§]

Department of Physical Chemistry and The Farkas Center for Light Induced Processes, The Hebrew University of Jerusalem, Givat-Ram, Jerusalem 91904, Israel

Received: October 24, 1996; In Final Form: January 3, 1997[⊗]

Insertion complexes of various bases with the protonated acetonitrile and acetone dimers have been studied using density functional methods including exact exchange contributions. The insertion mechanism has been investigated using an intrinsic reaction coordinate calculation. For some thermochemical quantities, calibration studies using larger basis sets and coupled cluster methods have been carried out. We find that B3LYP/cc-pVDZ will somewhat overestimate association energies due to basis set incompleteness error, which is partially compensated by an opposite error in the correlation treatment. B3LYP/4-21G will yield qualitatively correct structures, which PM3 and HF/4-21G generally do not, yielding instead asymmetric insertion complexes. The insertion energy increases with increasing proton affinity of the inserting base, while the association energy between the protonated central base and the ligands decreases. For the insertion complexes of the acetone dimer, the conformational equilibrium shifts from syn−syn to syn−anti with increasing proton affinity. The r_e geometries of protonated acetone dimer and its complexes are found to exhibit slight deviations from their intuitive symmetry that the calculations predict will be absent in the r_0 geometries. Computed association and switching enthalpies are in very good agreement with experiment, while proton transfer enthalpies fare less well due to the change in hydrogen bond number involved. Geometries and vibrational frequencies for all structures considered are available as Supporting Information to the paper.

I. Introduction

We have studied in recent years a series of reactions of proton-bound dimers in the gas phase.[1−7] A general pattern for the reactions of small proton-bound clusters with bases has been observed: fast reactions at near gas kinetic collision rate constants for proton-bound dimers and trimers such as $(RCOOH)_nH^+$ (n = 2, 3) and $(ROH)_nH^+$ (n = 2, 3) (R = H, CH_3) and slow reactions for alkyl blocked dimers and trimers such as $(CH_3CN)_2H^+$, $(CH_3COCH_3)_2H^+$, $(CH_3OCH_3)_2H^+$, and $(C_2H_5OH)(CH_3CN)_2H^+$. The different behavior of the two groups of cluster ions was ascribed to the ability of base molecules to hydrogen bond to a molecule in the periphery of the former cluster ion series and the inability to do so with the latter. A base molecule was presumed to attack the central proton of an alkyl blocked dimer in a T-shaped approach. A unique insertion reaction has been observed[2] for some alkyl blocked dimers such as $(CH_3CN)_2H^+$ and $(CH_3COCH_3)_2H^+$ with base molecules having hydrogen-bonding protons such as NH_3, CH_3NH_2, $(CH_3)_2NH$, and CH_3OH capable of forming a multiply hydrogen-bonded core ion. Trimethylamine, $(CH_3)_3N$, although having a higher proton affinity than ammonia, methylamine, dimethylamine, or methanol, does not undergo any association reaction with either $(CH_3CN)_2H^+$ or $(CH_3COCH_3)_2H^+$. A two-step mechanism was proposed:[2] (1) attack on the proton of the O−H−O or N−H−N bridge by the lone pair nitrogen or oxygen electrons and (2) rearrangement to a Y-shaped trimer structure. Trimethylamine is unable to undergo the second step of the mechanism proposed and as a result does not insert.

We have undertaken a density functional theoretical (DFT) study in order to learn about the structure and energetics of the reactant proton-bound dimers, $(CH_3CN)_2H^+$ and $(CH_3COCH_3)_2H^+$, and of the insertion product trimers with amines or methanol, and in order to verify the proposed insertion mechanism. The dimers $(CH_3CN)_2H^+$ and $(CH_3COCH_3)_2H^+$ are known to be particularly stable because they do not possess hydrogens that can form stable hydrogen-bonding networks beyond the dimer. The special stability of some of these dimers has been demonstrated by quantum mechanical calculations.[8−10] Cluster ionization and fragmentation[11] has demonstrated that although there are higher proton-bound clusters $(CH_3CN)_nH^+$, no further closed shell is visible beyond the first shell for n = 2. Steric hindrance was invoked as the cause for the reduced abundance of the trimer compared to the dimer in acetone[8] because the third molecule has to bind in a T-shaped structure. The linear structure was found to be more stable than the T-shaped structure[9] for the protonated acetonitrile trimer. The thermochemistry, that is, $\Delta H°$, $\Delta G°$, and $\Delta S°$ of the clustering reactions, is known for acetonitrile[9] and acetone[12] from high-pressure mass spectrometry equilibrium studies. The DFT calculations can therefore be compared with experimental values for the dimers and extended for the mixed trimers.

II. Methods

All density functional calculations have been carried out using the Gaussian 94 package[13] running on a DEC Alpha TurboLaser 8400 at the Institute of Chemistry, Hebrew University. Semiempirical calculations using the PM3 model[14] were also performed using this package. All conventional ab initio calculations were carried out using MOLPRO 96[15] running on the same computational hardware.

All density functional calculations employed the B3LYP (Becke three-parameter Lee−Yang−Parr) exchange−correlation functional,[16,17] which combines the Becke three-parameter exchange functional[16] with the gradient-corrected correlation functional of Lee, Yang, and Parr.[17] The excellent performance of this method for geometries and harmonic frequencies has been noted previously (e.g. refs 18, 19).

* To whom correspondence should be addressed.
[†] Present address: Department of Organic Chemistry, Kimmelman Building, Room 262, Weizmann Institute of Science, Rehovot 76100, Israel.
[‡] Boğaziçi Universitesi, F. E. F Kimya, Bebek 80815 Istanbul, Turkey.
[§] Archie and Marjorie Sherman Professor of Chemistry.
[⊗] Abstract published in *Advance ACS Abstracts,* February 15, 1997.

S1089-5639(96)03308-7 CCC: $14.00

TABLE 1: Convergence of Proton Affinity (kcal/mol) and Protonated Dimer Dissociation Energy (kcal/mol) of Acetonitrile and Acetone with Respect to (One-Particle) Basis Set and *n*-Particle (Correlation) Treatment

	acetonitrile		acetone	
	PA	$D_e(AH^+\cdots A)$	PA	$D_e(AH^+\cdots A)$
B3LYP/cc-pVDZ	194.47	35.21	205.15	35.00
with BSSE correction	192.85	32.80	203.53	31.39
B3LYP/cc-pVTZ	195.04	32.53	204.25	32.00
with BSSE correction	194.60	31.96	203.61	30.95
B3LYP/aug-cc-pVTZ	194.45	32.19		
HF/cc-pVDZ	195.02	27.96	207.98	27.32
MP2/cc-pVDZ	190.89	34.70	201.36	34.37
CCSD/cc-pVDZ	193.30	32.30	204.50	32.38
CCSD(T)/cc-pVDZ	193.12	33.42	203.83	33.53
best estimate[a]	193.25	30.17	202.93	29.48
zero-point contribution	−6.59	+0.60	−7.96	+0.82
best estimate at 0 K	186.66	30.77	194.33	30.30
at 298 K (ΔE)	186.44	30.22	194.33	29.51
at 298 K (ΔH)	187.03	30.81	194.92	30.10
experiment	188.4 ± 2[48]	29.8 ± 1.0[9]	193.7 ± 0.6[49]	30.1 ± 1.0[12]

[a] In the "hypothetical motionless state".

Apart from the standard 4-21G basis set,[20] all basis sets employed belong to the correlation consistent[21,22] family of Dunning and co-workers. The first one, cc-pVDZ (correlation consistent polarized valence double ζ), is a [3s2p1d/2s1p] contraction of a (9s4p1d/4s1p) basis set. The second, cc-pVTZ (correlation consistent polarized valence triple ζ), is a [4s3p2d1f/3s2p1d] contraction of a (10s5p2d1f/5s2p1d) basis set. The third one, aug-cc-pVTZ (augmented cc-pVTZ), additionally carries one low-exponent basis function of each angular momentum to accommodate anions, highly polar molecules, and weak molecular interactions.

To assess the quality of the B3LYP correlation treatment, CCSD(T),[23,24] or coupled cluster with all single and double substitutions[25] and a quasiperturbative treatment of connected triple substitutions,[23] calculations were carried out using the cc-pVDZ basis set and from B3LYP/cc-pVDZ reference geometries.

Finally, an approximate correction for basis set superposition error for the dimers was attempted using the familiar Boys−Bernardi counterpoise method.[26]

III. Results and Discussion

A. Calibration of the Method. Computed results for the PAs (proton affinities) of acetonitrile and acetone, as well as the dissociation energies of the corresponding protonated dimers, are given in Table 1, together with the relevant experimental values.

The results for the protonated dimer D_e values (dissociation energies) are both about 5 kcal/mol higher than experiment at the B3LYP/cc-pVDZ level. Taking the zero-point energy into account actually increases the gaps by 0.60 and 0.82 kcal/mol, respectively. While the rigid rotor-harmonic oscillator approach for the thermodynamics is of very limited value in such floppy molecules, we may assume that the errors more or less cancel in the dimerization reaction. If so, the thermal contribution actually nearly cancels out with the zero-point contribution.

There are three obvious candidates for the cause of the error: (a) basis set incompleteness; (b) (relatedly) basis set superposition error (BSSE); (c) inadequate electron correlation method.

Extending the basis set from cc-pVDZ to cc-pVTZ lowers D_e by 2.68 kcal/mol for acetonitrile and 3.00 kcal/mol for acetone. A further extension to the aug-cc-pVTZ basis set for acetonitrile lowers the value by a further 0.34 kcal/mol; the corresponding calculation for the protonated acetone dimer proved beyond our computational resources.

Because of the very appreciable change in geometry upon protonation (particularly, in the proton−base distance), all calculations involved in determining the basis set superposition error were carried out at the product geometry, including the monomer calculations:

$$\mathrm{BSSE} = E[\mathrm{A(B)}] + E[\mathrm{(A)B}] - E[\mathrm{A}] - E[\mathrm{B}] \qquad (1)$$

where E[A(B)] stands for the energy of A with the basis set of B added as "ghost" basis functions, and all atoms were kept at their positions from the E[AB] calculation.

For the B3LYP/cc-pVDZ calculations, the counterpoise corrections amount to 2.41 kcal/mol for the protonated acetonitrile dimer and 3.61 kcal/mol for the protonated acetone dimer. For the B3LYP/cc-pVTZ basis set, however, these numbers drop to 0.57 and 1.05 kcal/mol, respectively. This largely offsets the fairly big difference between the uncorrected results with the cc-pVDZ and cc-pVTZ basis sets.

From comparing CCSD(T) and B3LYP results with the cc-pVDZ basis set, it seems that the B3LYP exchange−correlation functional overestimates the protonated dimer D_e for acetonitrile by about 1.79 kcal/mol and that of acetone by about 1.47 kcal/mol. It should be noted that this is on the same order of magnitude as the effect of the triple excitations contribution: 1.12 and 1.15 kcal/mol, respectively. The total correlation energy contribution to D_e is fairly significant: 5.46 kcal/mol for $(CH_3CN)_2H^+$ and 6.21 kcal/mol for $(CH_3COCH_3)_2H^+$, or about one-fifth of the total. MP2 overestimates the correlation contributions by 1.28 and 0.84 kcal/mol, respectively, while CCSD, of course, underestimates them by 1.12 and 1.15 kcal/mol, respectively.

We can now define a "best estimate" energy as follows.

$$E = E[\mathrm{B3LYP/cc\text{-}pVTZ}] + E[\mathrm{CCSD(T)/cc\text{-}pVDZ}] - E[\mathrm{B3LYP/cc\text{-}pVDZ}] - \mathrm{BSSE} \qquad (2)$$

Thus we obtain values in the hypothetical motionless state of 30.17 kcal/mol for the protonated acetonitrile dimer and 29.48 kcal/mol for the protonated acetone dimer. After bringing zero-point and thermal corrections into account, we finally obtain values of 30.81 and 30.10 kcal/mol, respectively. The former is 1 kcal/mol higher than experiment (which is on the borderline of the experimental error bar); the latter agrees to the first decimal place.

Best estimates for the proton affinities can be obtained likewise. Again, both values thus obtained are in very good agreement with experiment.

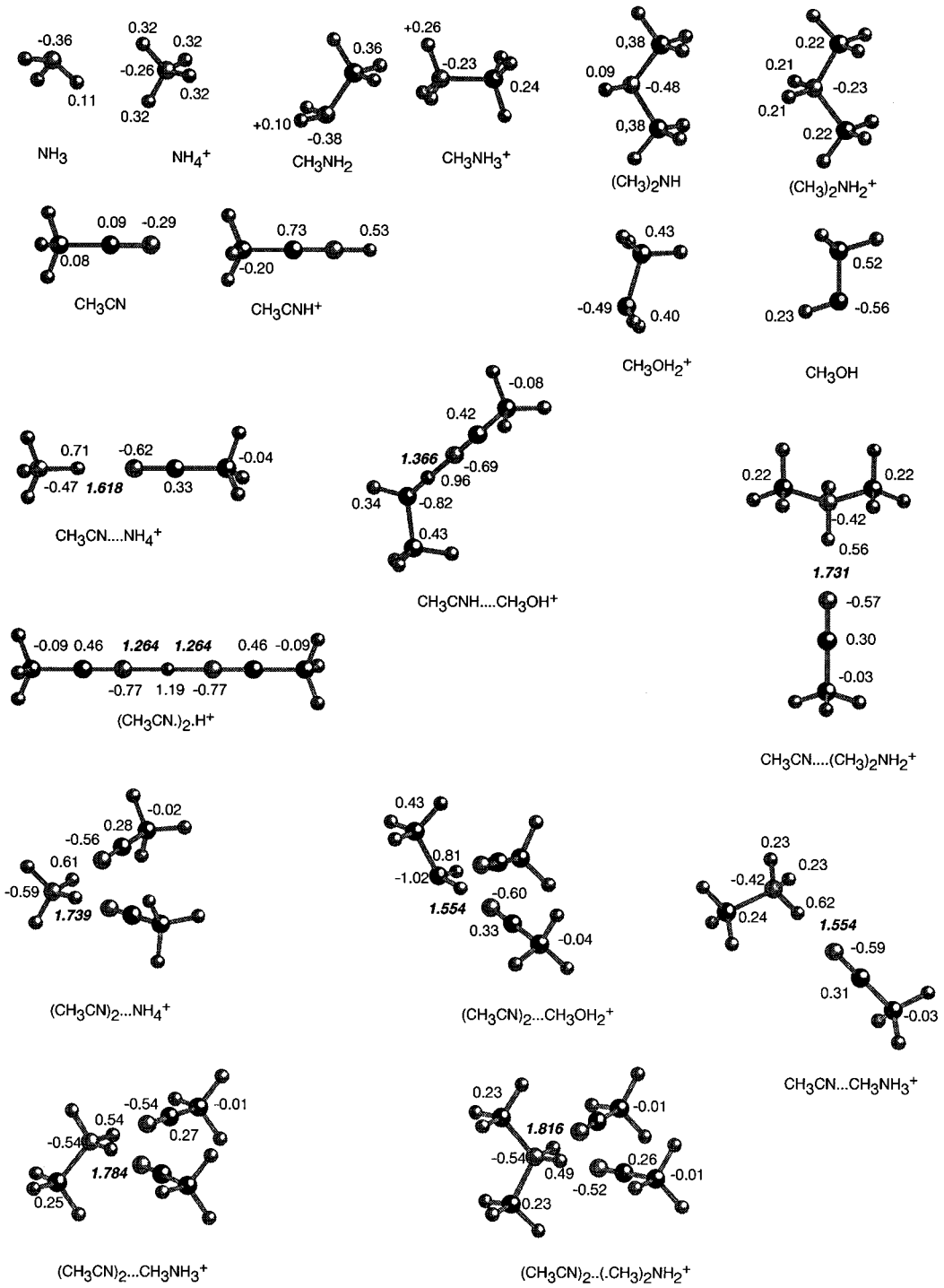

Figure 1. Overview of structures for the insertion complexes of the protonated acetonitrile dimers. APT charges and hydrogen bond distances at the B3LYP/cc-pVDZ level are shown in plain and italic numbers, respectively.

In conclusion, we can state that B3LYP/cc-pVDZ calculations of association energies on the other species will be too high by about 5 kcal/mol, of which about two-thirds will be due to basis set incompleteness (of which, plainly, BSSE is yet another manifestation) and the remainder due to inadequacies in the electron correlation treatment.

As for the harmonic frequencies for the various species and the reliability of the derived zero-point energies, we will consider four molecules in detail: CH_3OH, CH_3CN, CH_3NH_2, and CH_3COCH_3.

The computed harmonic frequencies for methanol agree quite well with the experimental fundamentals[27] for the "pure" vibrational modes $\nu_1-\nu_{11}$, except for the CH and OH stretches, where the discrepancy is consistent with the expected (large) anharmonicity for such modes. ν_{12}, the internal rotation of the CH_3 and OH groups with respect to each other, is subject to strong coupling with the overall rotation, and therefore the listed fundamental is only indicative.[28]

For CH_3CN, a series of high-resolution IR measurements (e.g. refs 29, 30, 31) have recently been performed, aside from the older work of Duncan and co-workers.[32] The present B3LYP/cc-pVDZ calculations reproduce the experimental frequencies remarkably well, considering the comparatively low level of theory. For the CH stretching bands ν_1 and ν_4, the difference between calculated ω and observed ν is consistent with the expected anharmonicity. The discrepancy for the CN stretching

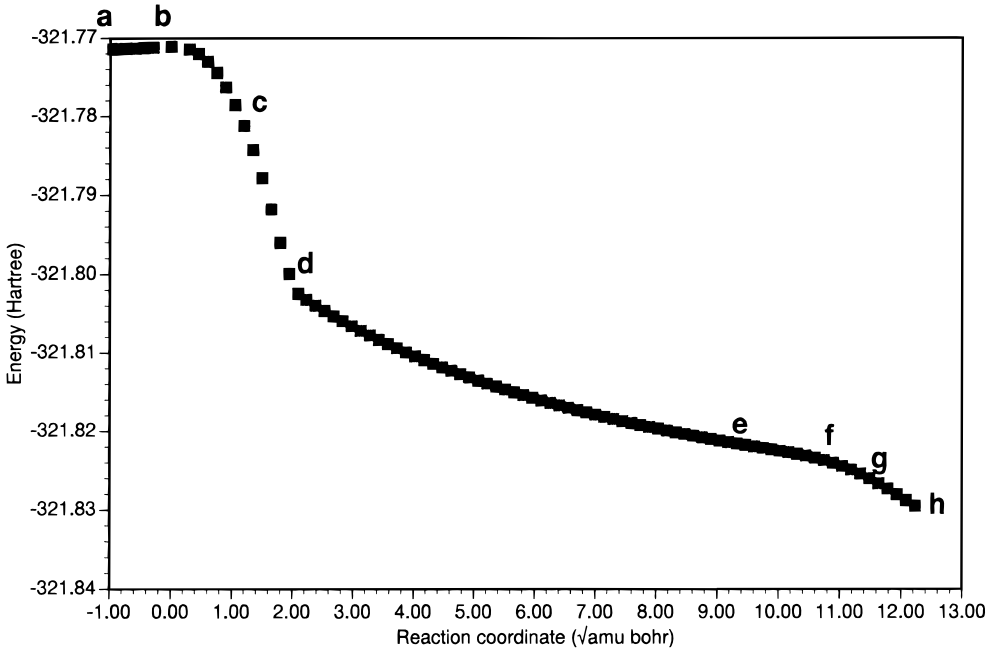

Figure 2. Profile of the B3LYP/4-21G reaction coordinate for the insertion of NH_3 into the acetonitrile dimer.

band ν_2 lies well beyond reasonable anharmonicity and is due partly to a known deficiency of B3LYP for high bond orders[18] and partly to a strong Fermi type 2 resonance with $\nu_3 + \nu_4$.

For CH_3NH_2, experimental values are taken from refs 33 and 34. The only discrepancies out of the ordinary between calculated ω_i and observed ν_i are found for ν_9 (the NH_2 wag, which exhibits inversion doubling) and ν_{15} (the CH_3 internal rotation). Neither is expected to be well reproduced by a harmonic-only frequency calculation to begin with: this limitation should be kept in mind for the other species. (Good DFT results for this molecule were previously obtained in, for example, ref 35.)

For acetone, experimental values are taken from refs 36−38. The only vibration that poses significant problems is ν_{12}, the antisymmetric combination of the CH_3 torsions; the symmetric combination is fortuitously well reproduced.

These sorts of problems may compromise the accuracy of computed absolute zero-point energies and thermodynamic properties; however, when considering, for example, differences between dimer and monomer, or unprotonated and protonated species, it can be assumed that these effects largely cancel.

Since the harmonic frequencies of the remaining species, particularly the protonated ones, are not really germane to the present discussion but may be useful to assist future experimental work, they are made available as Supporting Information to the present paper. Infrared intenstities are also made available there: from a recent study by De Proft et al.,[39] it is known that B3LYP/cc-pVDZ intensities are generally in at least semiquantitative agreement with experiment.

B. Insertion Complexes. *1. Acetonitrile.* All relevant structures are depicted in Figure 1. Full geometry information is available as Supporting Information to the present work; bond lengths for the hydrogen bonds are provided in the figure, as are the APT (atomic polarizability tensor[40]) atomic charges of all atoms except the methyl hydrogens. (All the charges are given along with the geometries in the Supporting Information.) As shown previously,[39,41] B3LYP/cc-pVDZ APT charges are close to convergence in both basis set and electron correlation method.

As expected, protonated acetonitrile (methyl cyanide) has C_{3v} symmetry like the unprotonated structure. The protonated dimer is found to have D_{3d} symmetry, with a linear $CN\cdots H^+\cdots NC$ arrangement, the proton midway, and the two methyl groups staggered. It should be noted that the methyl group internal rotations in this complex will be essentially free at room temperature. The dissociation energy of the protonated dimer is calculated as 35.3 kcal/mol at the B3LYP/cc-pVDZ level.

(Cybulski and Scheiner[42] found that, at the SCF level, the proton in $(CN\cdots H\cdots NC)^-$ is placed off-center. Repeating their calculations at the B3LYP level, however, leads to a centrosymmetric structure, consistent with the present results.)

An NH_3 molecule was then placed in a T-shaped arrangement with the free electron pair directed toward the protonated dimer in its staggered conformation (one of the hydrogens perpendicular to the NHN plane, resulting in no symmetry at all), and a transition-state search was carried out. The resulting stationary point exhibits one imaginary frequency (323i) at the B3LYP/4-21G level. To ascertain that it indeed belonged to the reaction coordinate of interest, an IRC (intrinsic reaction coordinate) calculation[43,44] was then carried out. A profile of the reaction coordinate is given in Figure 2, while an overview of some salient structures thereof is given in Figure 3.

In the reverse direction, the IRC leads to an ion−dipole complex, as expected. In the forward direction, the structure at first seems to lead to the products of the switching reaction, but as one proceeds further along the reaction coordinate, the hydrogens in the ammonia group undergo torsion, leading eventually to a bridged structure and finally a Y-shaped insertion complex in which two protons on NH_4^+ each are hydrogen-bonded to one CH_3CN molecule. This "bridged complex", which has C_{2v} symmetry, is considerably lower in energy (10.7 kcal/mol at the B3LYP/cc-pVDZ level) than the T-shaped structure. The numerical experiment just described reveals the exact mechanism proposed in ref 2 and described in the Introduction. Computer time limitations precluded carrying out the IRC calculation (which involved some 300 gradient calculations in the forward direction alone) at the B3LYP/cc-pVDZ level, but since we found in the present work that B3LYP/4-21G and B3LYP/cc-pVDZ are in at least qualitative agreement for the structures considered, we see no reason why the results of a B3LYP/cc-pVDZ IRC calculation would be appreciably different.

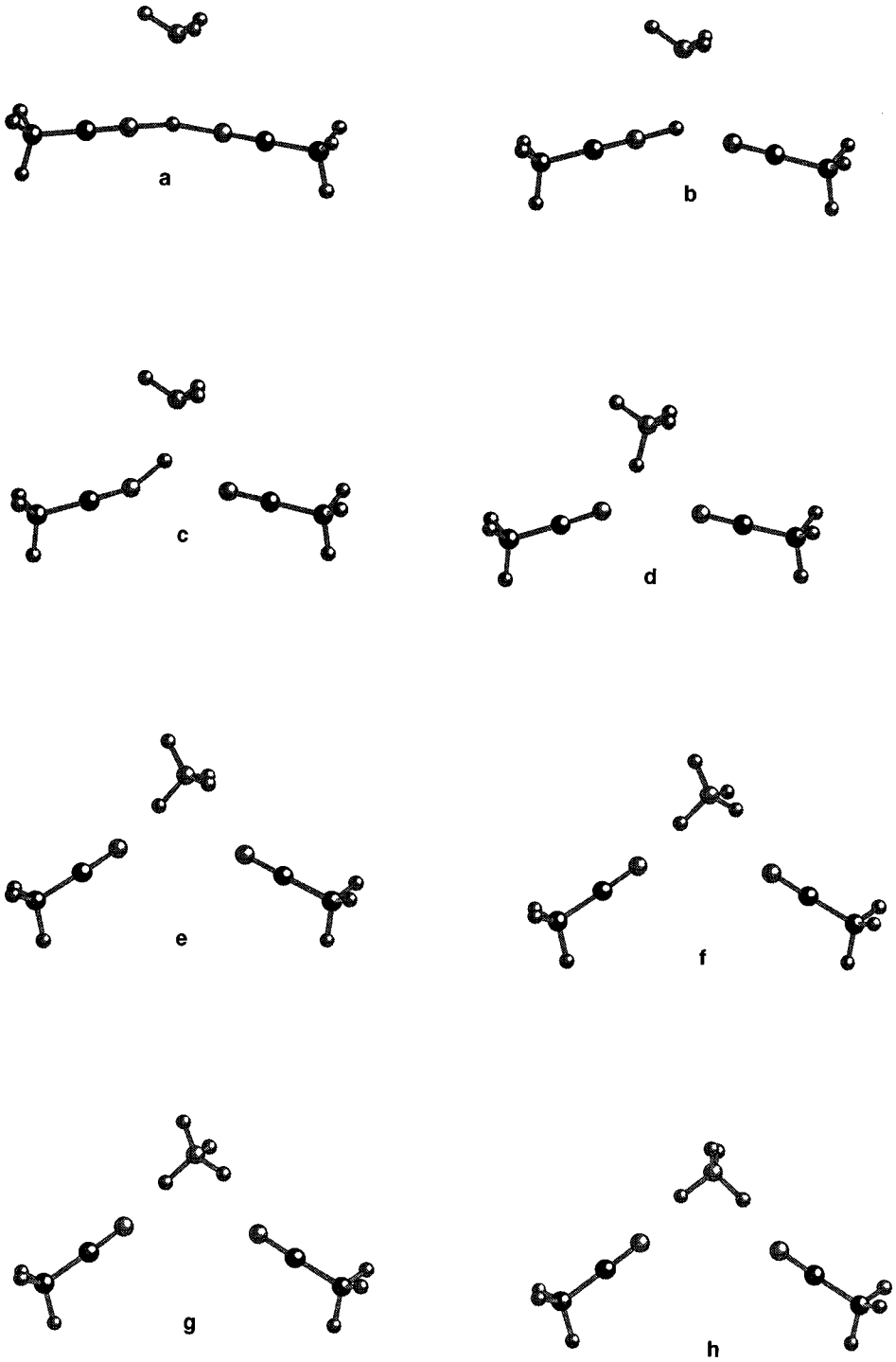

Figure 3. Some salient structures along the reaction coordinate for insertion of NH_3 into the protonated acetonitrile dimer.

We did recalculate the structures of the entrance channel ion−dipole complex and of the transition state at the B3LYP/cc-pVDZ level. The former is found to be 6.79 kcal/mol below the reactants in the hypothetical motionless state (HMS) and 5.38 kcal/mol at 0 K. The $H_3N\cdots H$ distance is found to be about 2.72 Å, while the two methyl groups are in nearly perfectly *geschrankte* conformations. The transition state still lies 4.89 kcal/mol (HMS) or 2.78 kcal/mol (0 K) below the reactants, while the products are a respectable 39.26 kcal/mol (HMS) or 33.90 kcal/mol (0 K) below the reactants. The imaginary frequency for the reaction coordinate at the transition state was found to be 465i cm^{-1}.

The dissociation energy of the insertion complex into $NH_4^+ + 2CH_3CN$ is found to be 52.2 kcal/mol at the B3LYP/cc-pVDZ level, which is somewhat less than twice the dissociation energy of the mixed dimer cation $NH_4^+\cdots NCCH_3$, 29.9 kcal/mol. This underscores that, rather than a solvation complex of the mixed dimer, the mixed trimer represents a situation with two equivalent strong hydrogen bonds of somewhat lower strength than an isolated single one.

If this view were correct, experimentally one would observe such protonated trimers $CH_3CN\cdots BH^+\cdots NCCH_3$ for $B = NH_3$, NH_2R, and NHRR′, but not for NRR′R″: as noted in the Introduction, the trimer is observed experimentally with ammonia, methylamine, and dimethylamine, but not with trimethylamine.

We have considered insertion complexes with a number of other "insertors". A summary of the computed thermochemical

TABLE 2: Comparison of Computed (B3LYP/cc-pVDZ) Harmonic Frequences (cm^{-1}) and Observed Fundamentals (cm^{-1}) for Methanol, Acetonitrile, Methylamine, and Acetone

	CH_3OH
experiment[27]	
a′	3681.5, 2999.0, 2844.3, 1477, 1454.3, 1340, 1074.5, 1033.5
a″	2970, 1465, 1145, 295[a]
B3LYP/cc-pVDZ	
a′	3779.5, 3101.4, 2964.1, 1485.2, 1467.6, 1378.3, 1091.3, 1061.7
a″	3008.0, 1465.8, 1155.4, 336.0
	CH_3CN
experiment	
A	2953.92,[32] 2266.45,[32] 1385.171(23),[29] 920.290284(13)[31]
E	3009.16,[32] 1449.728(26),[29] 1041.854706(28),[31] 365.015965(12)[30]
B3LYP/cc-pVDZ	
A	3128.8, 2371.3, 1388.7, 938.7
E	3047.5, 1443.4, 1044.2, 384.4
	CH_3NH_2
experiment[33]	
a′	3360, 2962, 2820, 1623, 1474, 1430, 1130, 1044, 780[a]
a″	3424, 2985, 1485, 1335,[34] 972,[34] 264
B3LYP/cc-pVDZ	
a′	3453.5, 3051.2, 2943.0, 1652.3, 1470.7, 1441.3, 1170.1, 1068.4, 871.8
a″	3524.7, 3091.5, 1491.4, 1348.3, 978.5, 329.6
	CH_3COCH_3
experiment[36−38]	
a_1	3004, 2937, 1731, 1435, 1355, 1072, 777, 385
a_2	2972, 1426, 872, 112
b_2	3018, 2920, 1410, 1364, 1216, 891, 530
b_1	2972, 1454, 1090, 484, 130
B3LYP/cc-pVDZ	
a_1	3152.4, 3032.7, 1811.7, 1437.8, 1361.3, 1070.9, 789.4, 376.4
a_2	3089.9, 1435.4, 869.3, 36.0
b_2	3151.6, 3025.8, 1427.1, 1370.4, 1229.2, 879.6, 531.1
b_1	3097.0, 1458.4, 1104.1, 488.8, 146.3

[a] This fundamental is not well-defined due to strong coupling between internal and overall rotations. The listed value is the recommended one of Shimanouchi.[28]

data is given in Table 4 for the association, switching, and proton transfer reactions, together with the available experimental data (compiled in ref 2) and the experimental branching ratios.[2] Some ancillary thermochemical data are given in Table 5.

A number of trends can be seen in these tables. For instance, with increasing proton affinity in the series $B = NH_3 < CH_3NH_2 < (CH_3)_2NH$, the first and second association energies—that is, the energy changes of the reactions $BH^+ + A \rightarrow ABH^+$ and $ABH^+ + A \rightarrow A_2BH^+$, respectively—decrease, somewhat more notably so for the first than for the second association energy. As a result, the overall association energy of the base decreases with increasing proton affinity. This may be clarified by the following thermodynamic cycle:

$$\begin{array}{ccc} BH^+ + 2A & \xrightarrow{-D_1} & ABH^+ + A \\ -PA(B)\uparrow & & \downarrow -D_2 \\ 2A + B + H^+ & & A_2BH^+ \\ -PA(A)\downarrow & & \uparrow \Delta E_{\text{insertion}} \\ AH^+ + A + B & \xrightarrow{-D_3} & A_2H^+ + B \end{array} \qquad (3)$$

Inspection of the computed geometries reveals that the increasing proton affinity is itself linked to an increasing H···NC hydrogen bond distance. In the insertion energy—that is, the energy change of the reaction $A_2H^+ + BH \rightarrow (A\cdots H)_2B^+$—we see a slight increase with increasing PA, thanks to a compensation between the loss of association energy and the somewhat larger difference in proton affinities.

Considering that the cooperativity factor

$$r_c = \frac{\Delta E[A_2BH^+ \rightarrow 2A + BH^+]}{2\Delta E[ABH^+ \rightarrow A + BH^+]} \qquad (4)$$

is less than unity, anticooperativity appears to be present. r_c appears to be linearly correlated with PA(B), consistent with theories presented in the literature.[45]

It should be noted that the impact of the zero-point energy is fairly appreciable: it reduces the insertion energies by about 5 kcal/mol.

For $BH{=}CH_3OH$, we also calculate such a Y-shaped insertion complex (with C_s symmetry) to have a dissociation energy into $MeOH_2^+ + 2CH_3CN$ of 66.1 kcal/mol and into $CH_3CNH^+ + MeOH + CH_3CN$ of 62.5 kcal/mol. (This difference reflects the somewhat higher proton affinity of CH_3CN.) The energy for loss of a single CH_3CN is calculated to be 26.88 kcal/mol.

It may be of interest to compare the trends in the branching ratios between association, switching, and proton transfer observed experimentally[2] with the exothermicities for these reaction channels based on the calculations in Tables 4 and 5. The experimental trends (summarized in Table 4) are clearly consistent with the DFT calculations.

Agreement with the limited experimental association and switching enthalpies is as good as can reasonably be expected for this comparatively low level of theory (B3LYP/cc-pVDZ). For the proton transfer reaction, the agreement between theory and experiment is decidedly less good and seems to deteriorate as the PA of the inserting base decreases. This phenomenon is undoubtedly related to the fact that the proton transfer reaction involves a change in the number of hydrogen bonds, while their number is conserved in the association and switching reactions.

TABLE 3: Overview of Stationary Points for the Species Considered in the Present Paper

species	*E*(B3LYP/cc-pVDZ) (hartrees)	ZPE (kcal/mol)	point group	Hessian index[a]
CH_3CN	−132.761 505 8	28.23	C_{3v}	0
CH_3CNH^+	−133.071 416 1	34.82	C_{3v}	0
$CH_3CN\cdots H^+\cdots NCCH_3$	−265.889 120 2	62.45	D_{3d}	0
$CH_3CN\cdots NH_4^+$	−189.708 924 8	59.80	C_3	0
NH_3	−56.554 254 7	21.37	C_{3v}	0
NH_4^+	−56.899 711 6	30.72	T_d	0
CH_3NH_2	−95.858 029 2	39.87	C_s	0
$CH_3NH_3^+$	−96.218 775 1	49.38	C_s	0
$(CH_3)_2NH$	−135.166 469 4	57.49	C_s	0
$(CH_3)_2NH_2^+$	−135.536 358 9	67.30	C_{2v}	0
CH_3OH	−115.722 816 8	31.87	C_s	0
$CH_3OH_2^+$	−116.026 907 7	39.95	C_s	0
$CH_3OH\cdots H^+NCCH_3$	−248.850 939 5	67.91	C_1	0
$CH_3CN\cdots NH_4^+\cdots NCCH_3$	−322.505 946 6	89.18	C_{2v}	0
insertion transition state of same[b]	−322.451 173 9	85.93	C_1	1
entrance channel ion−dipole complex[c]	−322.454 190 3	85.23	C_1	0
$CH_3CN\cdots CH_3OH_2^+\cdots NCCH_3$	−381.655 273 8	97.80	C_s	0
$CH_3CN\cdots CH_3NH_3^+$	−229.022 992 6	78.30	C_1	0
$CH_3CN\cdots CH_3NH_3^+\cdots NCCH_3$	−361.817 561 4	107.34	C_s	0
$CH_3CN\cdots (CH_3)_2NH_2^+$	−268.337 297 5	96.13	C_s	0
$CH_3CN\cdots (CH_3)_2NH_2^+\cdots NCCH_3$	−401.130 142 2	125.08	C_{2v}	0
acetone	−193.164 301 6	51.99	C_{2v}	0
acetoneH$^+$	−193.491 036 6	59.87	C_s	1
acetoneH$^+$	−193.491 180 5	59.96	C_1	0
acetone$\cdots NH_4^+$	−250.111 504 4	83.32	C_s	2
acetone$\cdots NH_4^+$	−250.111 575 4	83.44	C_1	0
acetone$\cdots CH_3OH_2^+$ syn	−309.263 162 1	92.76	C_1	0
acetone$\cdots CH_3OH_2^+$ anti	−309.263 161 5	92.77	C_1	0
acetone$\cdots CH_3OH_2^+\cdots$acetone syn−syn	−502.465 527 8	145.32	C_s	0
acetone$\cdots CH_3OH_2^+\cdots$acetone syn−anti	−502.465 398 8	145.58	C_1	0
acetone$\cdots NH_4^+\cdots$acetone syn−syn	−443.309 976 9	136.50	C_{2v}	2
acetone$\cdots NH_4^+\cdots$acetone syn−syn	−443.310 022 1	136.69	C_s	0
acetone$\cdots NH_4^+\cdots$acetone syn−anti	−443.312 639 4	136.88	C_s	2
acetone$\cdots NH_4^+\cdots$acetone syn−anti	−443.312 683 3	137.06	C_1	0
acetone$\cdots H^+\cdots$acetone	−386.711 171 8	110.93	C_{2h}	2
acetone$\cdots H^+\cdots$acetone	−386.711 329 6	111.14	C_2	0
acetone$\cdots CH_3NH_3^+\cdots$acetone syn−syn	−482.620 367 4	154.84	C_s	1
acetone$\cdots CH_3NH_3^+\cdots$acetone syn−anti	−482.624 099 2	155.33	C_1	0
acetone$\cdots CH_3NH_3^+$	−289.425 856 2	102.19	C_1	0

[a] Number of negative eigenvalues of the Hessian. 0 means a minimum, 1 a transition state, 2 and more higher-order saddle points. [b] See Figure 3, structure b. [c] See Figure 3, structure a.

TABLE 4: Calculated and Observed Reaction Enthalpies (kcal/mol) and Observed[2] Branching Ratios (%) for Some Relevant Reactions

	association $A_2H^+ + B \rightarrow A_2BH^+$				switching $A_2H^+ + B \rightarrow ABH^+ + A$				proton transfer $A_2H^+ + B \rightarrow BH^+ + 2A$			
	calc ΔE_e	calc ΔE_0	expt ΔH	expt[a] ratio	calc ΔE_e	calc ΔE_0	expt ΔH	expt[a] ratio	calc ΔE_e	calc ΔE_0	expt[a] ΔH	expt[a] ratio
With Protonated Acetonitrile Dimer												
CH_3OH	−27.19	−23.71	−21[b]	95.3	−0.31	+1.5	+1[b]	4.7	+38.92	+41.01	+36.3	0
NH_3	−39.26	−33.9		70	−16.97	−12.77		30	+12.96	+16.32	+14.2	0
CH_3NH_2	−44.18	−39.16	−37.6[c]	62.3	−23.43	−19.22	−20.4[d]	37.3	+3.37	+6.5	+4.1	0.4
$(CH_3)_2NH$	−46.78	−41.64		42	−27.11	−22.69		51	−2.37	+1.45	−2.4	7
With Protonated Acetone Dimer												
CH_3OH	−19.69	−17.38			+4.19	+7.11			+49.34	+50.26	+44.9	
NH_3	−29.56	−25.01	−25.8[e]	60	−6.46	−3.54	−5.5[e]	40	+13.79	+16.44	+22.8	
CH_3NH_2	−34.35	−30.03	−28.1[d]	54	−13.05	−9.88	−11.3[c]	46	+8.06	+10.70	+12.7	<1

[a] Reference 2. [b] El-Shall, M. S.; Olafsdottir, S. R.; Mautner (Meot-Ner), M.; Sieck, L. W. *Chem. Phys. Lett.* **1991**, *185*, 193. El-Shall, M. S. Personal communication. [c] From relations between solvation enthalpies: Mautner (Meot-Ner), M. *J. Am. Chem. Soc.* **1984**, *106*, 1265. [d] Mautner (Meot-Ner), M. *J. Am. Chem. Soc.* **1984**, *106*, 1265. [e] Mautner (Meot-Ner), M. Private communication quoted in ref 2.

TABLE 5: Summary of B3LYP/cc-pVDZ Model Thermochemistry of the Insertion Complexes of Various Bases with Protonated Acetonitrile Dimer (kcal/mol)

	PA(B)		$A_2BH^+ \rightarrow ABH^+ + A$		$A_2BH^+ \rightarrow 2A + BH^+$		$ABH^+ \rightarrow A + BH^+$	
B	PA_e	PA_0	D_e	D_0	D_e	D_0	D_e	D_0
CH_3OH	190.82	182.74	26.88	25.21	66.11	64.72	39.23	39.50
a					62.46	59.58	35.58	34.36
NH_3	216.78	207.42	22.29	21.13	52.22	50.22	29.94	29.09
CH_3NH_2	226.37	216.86	20.75	19.94	47.55	46.05	26.80	26.11
$(CH_3)_2NH$	232.11	222.30	19.67	18.95	44.41	43.09	24.74	24.14

[a] Considering the formation of CH_3CNH^+ rather than $CH_3OH_2^+$ in the products.

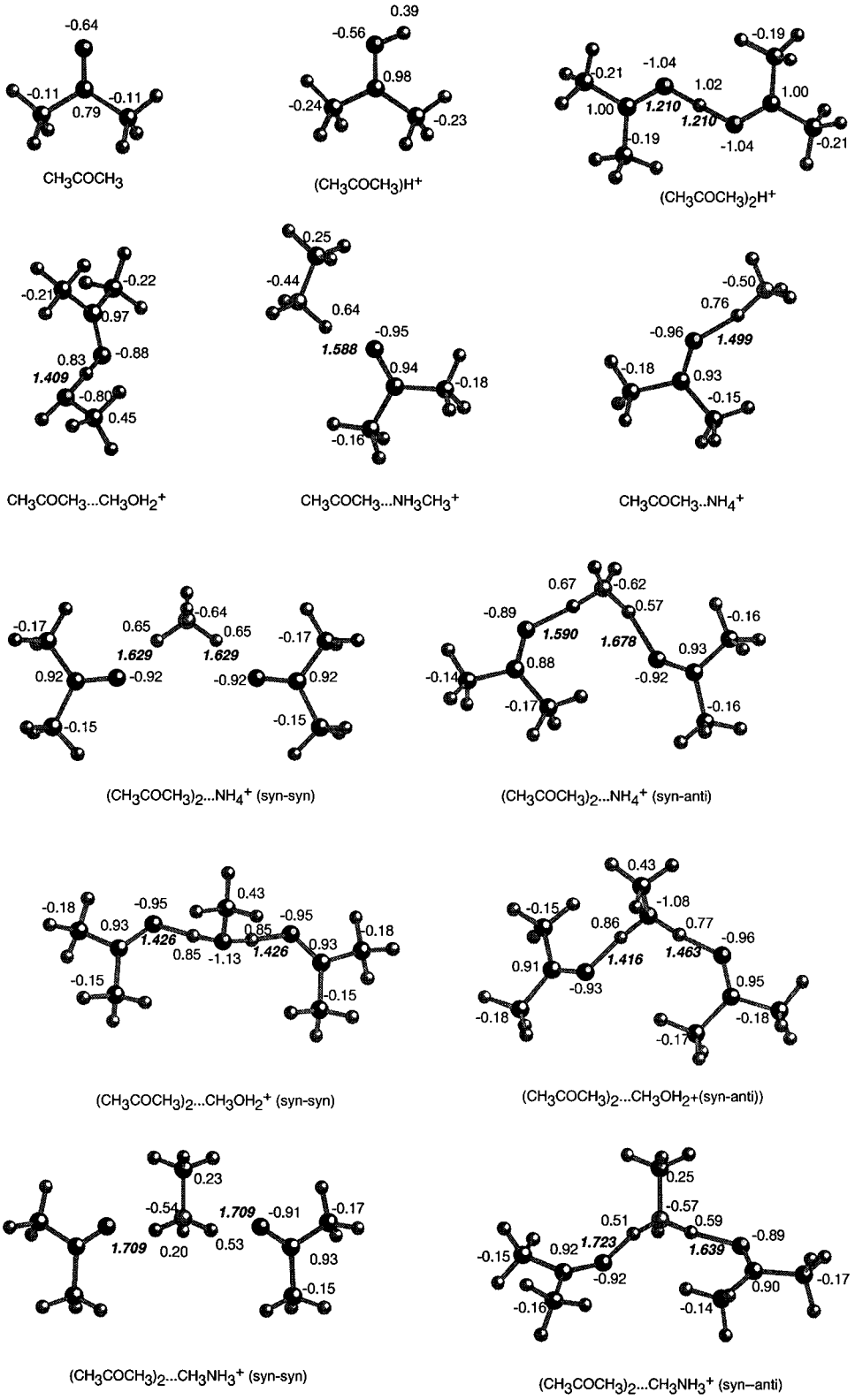

Figure 4. Overview of structures for the insertion complexes of the protonated acetone dimers. APT charges and hydrogen bond distances at the B3LYP/cc-pVDZ level are shown in plain and italic numbers, respectively.

It is noteworthy that while B3LYP/cc-pVDZ and B3LYP/4-21G consistently predict two equivalent hydrogen bonds, PM3 predicts two inequivalent ones, as do SCF/4-21G calculations. Therefore, both PM3 and HF/4-21G are essentially useless for generating starting geometries. In contrast, we found that B3LYP/4-21G geometries were consistently in at least semi-quantitative agreement with the B3LYP/cc-pVDZ ones and that the qualitative features of the various potential energy surfaces considered here were all well reproduced.

The fact that there is only a single H-bonding site on CH_3CN makes the situation relatively simple here from a conformational point of view. We will now proceed to the somewhat more complicated case of acetone.

2. Acetone. All relevant structures are depicted in Figure 4, together with the lengths of hydrogen bonds and APT charges for all atoms except the methyl hydrogens. Full geometry and APT charge information is again available as Supporting Information to the present work.

The expected full C_{2v} symmetry for acetone is found at all levels of theory considered: PM3, B3LYP/4-21G, and B3LYP/cc-pVDZ, with one hydrogen of each methyl group standing eclipsed toward the O atom. In protonated acetone, however, a repulsive interaction between the proton on the oxygen and the nearest H on a methyl group causes staggering of the methyl group by about 12°, leading to a minimum energy structure without any symmetry at all levels of theory. As expected, the energy lowering with respect to the C_s symmetric structure is very small (0.09 kcal/mol). We are therefore dealing with a symmetric double-well potential, where the central barrier height is on the same order of magnitude as the harmonic frequency at the bottom of the well. (This is illustrated by the fact that including the zero-point energy in the comparison—which essentially compares the barrier height and the zero-point energy level in the harmonic approximation—reduces the energy difference to 0.02 kcal/mol.) Under such circumstances, even at low temperatures rapid tunneling will take place, resulting in an averaged structure that approximately corresponds to the C_s "transition state". This kind of "quasisymmetric" structure—reminiscent of the "quasiplanar" structure in the water tetramer[46]—is a recurrent theme in the present section.

The structure one would expect for the protonated acetone dimer has C_{2h} symmetry. Because of the aforementioned steric interaction, reoptimizing without any symmetry lowered the total energy by 0.10 kcal/mol. However, the optimized structure exhibited C_2 symmetry (symmetric combination of the staggered conformations) to within the precision of the optimization. Actually, inclusion of zero-point energy changes the energetic ordering of the C_2 and C_{2h} structures and might suggest that even the r_0 geometry will have C_{2h} symmetry.

The dissociation energy of the protonated acetone dimer is found to be $D_e = 35.04$, $D_0 = 35.85$ kcal/mol at the B3LYP/cc-pVDZ level. While B3LYP clearly finds two equivalent proton−oxygen distances with both the 4-21G and cc-pVDZ basis sets, PM3 finds a spurious structure with the hydrogen tightly bound to one acetone and a weak hydrogen bond to the other acetone. Experimentation with SCF/4-21G and SCF/6-31G* calculations revealed the same phenomenon: we therefore conclude it is an artifact of the Hartree−Fock approximation.

Adding an NH_3 molecule to the complex results again in a bridged complex with two protons of NH_4^+ hydrogen-bonding to one acetone each. Because there are two lone pairs on the acetone oxygen, there are three distinct configurations for doing this: syn−syn, syn−anti, and anti−anti with respect to the two "free" hydrogens of the central NH_4^+. The anti−anti isomer leads to excessive steric hindrance between the methyl groups of the two acetones and was not considered further. The syn−syn conformer has C_s symmetry, being very slightly (0.03 kcal/mol at the B3LYP/cc-pVDZ level) distorted from the ideal C_{2v} geometry by the repulsive interaction noted for protonated acetone. Actually, inclusion of ZPE shifts the equilibrium by 0.19 kcal/mol toward the C_{2v} structure. The syn−anti conformer is notably lower in energy than the syn−syn one (1.70 kcal/mol): its r_e minimum energy conformation has no symmetry at all, the distorted geometry being 0.03 kcal/mol lower in energy than the ideal C_s structure. Once more, however, including ZPE makes the C_s structure the more stable one by a margin of 0.15 kcal/mol. The dissociation into $NH_4^+ + 2(CH_3)_2CO$ requires $D_e = 52.94$, $D_0 = 50.59$ kcal/mol at the B3LYP/cc-pVDZ level: the insertion reaction $[(CH_3)_2CO]_2H^+ + NH_3 \rightarrow (CH_3)_2CO\cdots NH_4^+\cdots OC(CH_3)_2$ yields $D_e = 29.56$, $D_0 = 25.02$ kcal/mol. The insertion complex is stable with respect to losing one acetone by a respectable $D_e = 23.10$, $D_0 = 21.40$ kcal/mol at the B3LYP/cc-pVDZ level.

Let us now consider the insertion complexes with methanol. Because the intrinsic symmetry of the syn−syn and syn−anti conformers is lowered to begin with (C_s and C_1, respectively), we only have to consider two stationary points. In the present case, the syn−syn conformer is actually lower in energy than the syn−anti conformer by 0.08 kcal/mol at the B3LYP/cc-pVDZ level. The dissociation energy into $CH_3OH_2^+ + 2(CH_3)_2CO$ is computed to be no less than $D_e = 69.04$, $D_0 = 67.39$ kcal/mol: the insertion reaction yields only $D_e = 19.69$, $D_0 = 17.12$ kcal/mol. This has everything to do with the fact that the proton affinity of methanol is lower than that of acetone. As for the loss of a single acetone from the bridged complex, that would require $D_e = 23.89$, $D_0 = 23.06$ kcal/mol.

For the insertion complex with methylamine, again only C_s syn−syn and C_1 syn−anti conformers have to be considered. Here, the syn−anti conformer is again lower than the syn−syn one by 2.33 kcal/mol. The dissociation into $CH_3NH_3^+ + 2(CH_3)_2CO$ requires $D_e = 48.1$, $D_0 = 46.2$ kcal/mol at the B3LYP/cc-pVDZ level; the insertion reaction yields $D_e = 34.34$; $D_0 = 30.02$ kcal/mol. The loss of a single acetone would require $D_e = 21.30$, $D_0 = 20.14$ kcal/mol.

Comparing these results reveals trends similar to those for the acetonitrile case. As the proton affinity of the "insertor" increases, the energy required for acetone loss decreases, which is consistent with the observation that the O···H hydrogen bond lengths become longer. Overall, the energy gain of the insertion reaction still increases, but not as rapidly as the proton affinity due to the concomitant loss in hydrogen bond strength.

It is interesting to note that the syn−anti conformer is apparently stabilized with respect to the syn−syn conformer as the PA increases. Some inspection of the O···H hydrogen bond lengths turns out to be rather informative.

For the CH_3OH insertion complex, rO···H in syn−syn is 1.426 Å, compared to RO···H = 1.463 and 1.416 Å in the syn−anti conformer. The distance in the $CH_3OH\cdots{}^+HOC(CH_3)_2$ complex is 1.409 Å. If we use a simplistic model of two "local mode" Morse potentials for the hydrogen bonds, it would follow, all other things being equal, that the syn−anti situation represents an overall energy loss compared to the syn−syn situation. For the NH_3 insertion complex, r(O···H) in syn−syn is 1.629 Å, compared to RO···H = 1.678 and 1.590 Å in the syn−anti conformer. The distance in the $NH_4^+\cdots OC(CH_3)_2$ complex is 1.478 Å. The shorter of the two distances in the syn−anti conformer actually represents a significant energy gain compared to the syn−syn distance, since we are on the far side of the equilibrium distance. In the case of the CH_3NH_2 insertion complex, r(O···H) is 1.709 in the syn−syn case and 1.723 vs 1.639 in the syn−anti case. Following the same reasoning, there should be a significant net *gain* in energy in going from syn−syn to syn−anti, on account of the hydrogen bonds alone.

As it turns out, in the relatively tightly bound CH_3OH insertion complex, there is a certain degree of sterical crowding in the syn−anti conformer. As the hydrogen bonds become longer, there is more conformational "leeway", and the closer of the two acetones in the syn−anti conformer can actually approach somewhat more closely.

Finally let us turn to the thermochemical quantities (Table 4). As for the acetonitrile complexes, agreement with experiment is very good for the association and switching reaction (where the overall number of hydrogen bonds stays constant at 2) and decidedly less good—deteriorating with decreasing PA of the inserting base—for the proton transfer reaction (which involves the breaking of one hydrogen bond).

IV. Conclusions

The insertion complexes of the protonated acetonitrile and acetone dimers have been studied using density functional methods. We can summarize our conclusions as follows.

B3LYP/cc-pVDZ will somewhat overestimate association energies due to basis set incompleteness error, which is partially compensated by an opposite error in the correlation treatment. The method is more than adequate for calculating the zero-point energies of the species concerned.

While B3LYP/4-21G will yield qualitatively correct symmetric structures for the insertion complexes, HF/4-21G and the semiempirical PM3 method will not.

The mechanism proposed in ref 2 has been confirmed.

Quite stable insertion complexes are formed.

The insertion energy $\Delta E_e[A_2H^+ + B \rightarrow A_2BH^+]$ increases with increasing proton affinity of the inserting base, while the association energy between protonated central base and ligands, $\Delta E_e[BH^+ + 2A \rightarrow A_2BH^+]$, decreases.

For the insertion complexes of the acetone dimer, the conformational equilibrium shifts from syn−syn to syn−anti with increasing PA.

While the r_e geometries of protonated acetone and its complexes exhibit small distortions from their intuitive symmetry, these probably are absent in the r_0 and other effective geometries.

B3LYP/cc-pVDZ computed association ($A_2H^+ + B \rightarrow A_2BH^+$) and switching ($A_2H^+ + B \rightarrow ABH^+ + A$) enthalpies agree well with experiment, while computed proton transfer ($A_2H^+ + B \rightarrow BH^+ + 2A$) enthalpies—which involve breakage of a hydrogen bond—deteriorate as the PA of base B decreases.

Acknowledgment. J.M. is a Senior Research Associate ("Onderzoeksleider") of the National Science Foundation of Belgium (NFWO/FNRS) and acknowledges a Golda Meir Fellowship from the Hebrew University. V.A. is grateful to the Boğaziçi University Research Funds for supporting her visit to Hebrew University. This research was supported by The Israel Science Foundation founded by the Israel Academy of Sciences and Humanities.

Supporting Information Available: B3LYP/cc-pVDZ Cartesian coordinates of all the species concerned and B3LYP/cc-pVDZ harmonic frequencies and IR intensities (19 pages); molecular movie in XMol format[47] (Internet only). Ordering information is given on any current masthead page. These items are also available on the Internet World Wide Web at the Uniform Resource Locator (URL) http://theochem.weizmann.ac.il/web/papers/insertion.html.

References and Notes

(1) Feng, W. Y.; Iraqi, M.; Lifshitz, C. *J. Phys. Chem.* **1993**, *97*, 3510.
(2) Feng, W. Y.; Goldenberg, M.; Lifshitz, C. *J. Am. Soc. Mass Spectrom.* **1994**, *5*, 695.
(3) Feng, W. Y.; Lifshitz, C. *J. Phys. Chem.* **1994**, *98*, 3658.
(4) Feng, W. Y.; Lifshitz, C. *Int. J. Mass Spectrom. Ion Processes* **1995**, *149/150*, 13.
(5) Feng, W. Y.; Lifshitz, C. *J. Mass Spectrom.* **1995**, *30*, 1179.
(6) Feng, W. Y.; Lifshitz, C. *J. Am. Chem. Soc.* **1995**, *117*, 11548.
(7) Feng, W. Y.; Ling, Y.; Lifshitz, C. *J. Phys. Chem.* **1996**, *100*, 35.
(8) Yamabe, S.; Makato, T.; Hirao, K. *Can. J. Chem.* **1983**, *61*, 2827.
(9) Deakyne, C. A.; Meot-Net (Mautner), M.; Campbell, C. L.; Hughes, M. G.; Murphy, S. P. *J. Chem. Phys.* **1986**, *84*, 4958.
(10) Aviyente, V.; Varnali, T. *J. Mol. Struct.* **1992**, *277*, 285.
(11) Mestdagh, J. M.; Binet, A.; Sublemontier, O. *J. Phys. Chem.* **1989**, *93*, 8300.
(12) Meot-Net (Mautner), M. *J. Am. Chem. Soc.* **1992**, *114*, 3312.
(13) Frisch, M. J.; Trucks, G. W.; Schlegel, H. B.; Gill, P. M. W.; Johnson, B. G.; Robb, M. A.; Cheeseman, J. R.; Keith, T.; Petersson, G. A.; Montgomery, J. A.; Raghavachari, K.; Al-Laham, M. A.; Zakrzewski, V. G.; Ortiz, J. V.; Foresman, J. B.; Cioslowski, J.; Stefanov, B. B.; Nanayakkara, A.; Challacombe, M.; Peng, C. Y.; Ayala, P. Y.; Chen, W.; Wong, M. W.; Andres, J. L.; Replogle, E. S.; Gomperts, R.; Martin, R. L.; Fox, D. J.; Binkley, J. S.; Defrees, D. J.; Baker, J.; Stewart, J. P.; Head-Gordon, M.; Gonzalez, C.; Pople, J. A. *GAUSSIAN 94, Revision B.1*; Gaussian, Inc.: Pittsburgh, 1995.
(14) Stewart, J. J. P. *J. Comput. Chem.* **1989**, *10*, 209.
(15) MOLPRO 96 is an ab initio MO package by Werner, H. J.; Knowles, P. J.; with contributions from Almlöf, J.; Amos, R. D.; Deegan, M. J. O.; Elbert, S. T.; Hampel, C.; Lindh, R.; Meyer, W.; Peterson, K. A.; Pitzer, R. M.; Stone, A. J.; Taylor, P. R.
(16) Becke, A. D. *J. Chem. Phys.* **1993**, *98*, 5648.
(17) Lee, C.; Yang, W.; Parr, R. G. *Phys. Rev.* **1988**, *B37*, 785.
(18) Martin, J. M. L.; El-Yazal, J.; François, J. P. *Mol. Phys.* **1995**, *86*, 1437.
(19) Finley, J. W.; Stephens, P. J. *J. Mol. Struct. (THEOCHEM)* **1995**, *357*, 225.
(20) Pulay, P.; Fogarasi, G.; Pang, F.; Boggs, J. E. *J. Am. Chem. Soc.* **1979**, *101*, 2550.
(21) Dunning, T. H., Jr. *J. Chem. Phys.* **1989**, *90*, 1007.
(22) Kendall, R. A.; Dunning, T. H., Jr.; Harrison, R. J. *J. Chem. Phys.* **1992**, *96*, 6796.
(23) Raghavachari, K.; Trucks, G. W.; Head-Gordon, M.; Pople, J. A. *Chem. Phys. Lett.* **1989**, *157*, 479.
(24) Hampel, C.; Peterson, K. A.; Werner, H. J. *Chem. Phys. Lett.* **1992**, *190*, 1.
(25) Purvis, G. D., III; Bartlett, R. J. *J. Chem. Phys.* **1982**, *76*, 1910.
(26) Boys, S. F.; Bernardi, F. *Mol. Phys.* **1970**, *19*, 553.
(27) Henningsen, J. O. In *Infrared and Millimeter Waves*; Button, K. J., Ed.; Academic Press: New York, 1982; Vol. V, Chapter 2.
(28) Shimanouchi, T. *Tables of Molecular Vibrational Frequencies, Consolidated Volume I*; National Bureau of Standards: Washington, DC, 1972.
(29) Paso, R.; Anttila, R.; Koivusaari, M. *J. Mol. Spectrosc.* **1994**, *165*, 470.
(30) Koivusaari, M.; Horneman, V.-M.; Anttila, R. *J. Mol. Spectrosc.* **1992**, *152*, 377.
(31) Tolonen, A.-M.; Koivusaari, M.; Paso, R.; Schroderus, J.; Alanko, S.; Anttila, R. *J. Mol. Spectrosc.* **1993**, *160*, 554.
(32) Duncan, J. L.; McKean, D. C.; Tullini, F.; Nivellini, G. D.; Pena, J. P. *J. Mol. Spectrosc.* **1978**, *69*, 123.
(33) Gray, A. P.; Lord, R. C. *J. Chem. Phys.* **1957**, *26*, 690.
(34) Hamada, Y.; Tanaka, N.; Sugawara, Y.; Hirakawa, A. Y.; Tsuboi, M. *J. Mol. Spectrosc.* **1982**, *96*, 313.
(35) Csonka, G. I.; Sztraka, L. *Chem. Phys. Lett.* **1995**, *233*, 611.
(36) Dellepiane, G.; Overend, J. *Spectrochim. Acta* **1966**, *22*, 593.
(37) Harris, W. C.; Levin, I. W. *J. Mol. Spectrosc.* **1972**, *43*, 117.
(38) Hollenstein, H.; Günthard, H. H. *J. Mol. Spectrosc.* **1980**, *84*, 457.
(39) De Proft, F.; Martin, J. M. L.; Geerlings, P. *Chem. Phys. Lett.* **1996**, *250*, 393.
(40) Cioslowski, J. *J. Am. Chem. Soc.* **1989**, *111*, 8333.
(41) De Proft, F.; Geerlings, P.; Martin, J. M. L. In *Density-Functional Methods in Chemistry*; Seminario, J., Politzer, P., Eds.; Elsevier: Amsterdam, 1996.
(42) Cybulski, S. M.; Scheiner, S. *J. Am. Chem. Soc.* **1987**, *109*, 4199.
(43) Fukui, K. *Acc. Chem. Res.* **1981**, *14*, 363.
(44) Gonzales, C.; Schlegel, H. B. *J. Chem. Phys.* **1989**, *90*, 2154; *J. Phys. Chem.* **1990**, *94*, 5523.
(45) Maes, G.; Smets, J. *J. Phys. Chem.* **1993**, *97*, 1818.
(46) Cruzan, J. D.; Braly, L. B.; Liu, K.; Brown, M. G.; Loeser, J. G.; Saykally, R. J. *Science* **1996**, *271*, 59.
(47) *XMol*, version 1.3.1; Minnesota Supercomputer Center, Inc.: Minneapolis MN, 1993. Available on the Internet at the URL ftp://ftp.msc.edu/pub/xmol.
(48) Lias, S. G.; Liebman, J. F.; Levin, R. D. *J. Phys. Chem. Ref. Data* **1980**, *13*, 695.
(49) Szulejko, J. E.; McMahon, T. B. *J. Am. Chem. Soc.* **1993**, *115*, 7839.